ACI MATERIALS JOURNAL TECHNICAL PAPER

Title No. 115-M12

Factorial Design and Optimization of Ultra-High-Performance Concrete with Lightweight Sand

by Weina Meng, V. A. Samaranayake, and Kamal H. Khayat

*In this study, lightweight sand is used as an internal curing agent in ultra-high-performance concrete (UHPC). A factorial design approach was employed to evaluate the effects of multiple mixture proportioning parameters that are important for mixture optimization of UHPC. The investigated mixture design parameters included the substitution volume ratio of lightweight sand for river sand (LWS/NS: 0 to 25%), the cementitious materials-to-sand volume ratio (*cm/s*: 0.8 to 1.2), and the water-cementitious materials ratio (*w/cm*: 0.17 to 0.23). The evaluated properties included fresh properties, compressive strengths at up to 91 days, and autogenous shrinkage at up to 28 days. Statistical models that take into account the coupling effects of mixture proportioning parameters were formulated to predict the UHPC properties. The* w/cm *and LWS/NS were the most significant parameters influencing the compressive strength and autogenous shrinkage, respectively. By replacing the river sand with 25% lightweight sand, the compressive strength at 91 days increased from 150 to 170 MPa (22.5 to 25.5 ksi) and the autogenous shrinkage at 28 days decreased from 410 to 70 μm/m (410 × 10^{-6} to 70 × 10^{-6} in./in.). The mixture with* w/cm *of 0.23, LWS/NS of 0.25, and* cm/s *of 1.2 is determined as the optimum UHPC mixture. The material properties of the mixture: the HRWR demand was 0.6%, the 28-day autogenous shrinkage was 260 μm/m (260 × 10^{-6} in./in.), and the 91-day compressive strength was 147 MPa (22.1 ksi).*

Keywords: autogenous shrinkage; compressive strength; factorial design; internal curing; lightweight sand; rheological properties; ultra-high-performance concrete (UHPC).

INTRODUCTION

Ultra-high-performance concrete (UHPC) is an advanced cementitious material with exceptional mechanical performance and improved durability compared with high-performance concrete.[1] The enhanced durability of UHPC can particularly benefit infrastructure that undergoes serious environmental loadings. However, because of the high contents of cement, quartz sand, and steel fibers used, the cost of UHPC is considerably higher than conventional concrete, which limits the extension of its application.[2] As a result, cost-effective UHPC mixtures prepared with a high volume of supplementary cementitious materials and conventional concrete sand were systematically developed by authors in a previous study.[3] A rheological control technique and nanomaterials were incorporated to further improve the mechanical properties of the UHPC mixtures.[4,5] However, under standard curing, the 28-day compressive strength of the cost-effective UHPC was limited to 130 MPa (19.5 ksi). Even though the autogenous shrinkage was substantially reduced compared with the reference mixture, it still remained as high as 550 μm/m (550 × 10^{-6} in./in.).[3] For UHPC, the water-cementitious materials ratio (*w*/*cm*) is normally less than 0.25, lacks water, and capillary pore space compromises the precipitation of hydration products, thus resulting in low degrees of hydration and limited strength.[6,7] Besides, the low *w*/*cm* leads to high self-desiccation, which tends to lead to cracks in UHPC.[8]

To increase cement hydration degree and decrease autogenous shrinkage, lightweight aggregates were employed as internal curing agents.[9-11] Bentz et al.[10] claimed that small, pre-saturated lightweight sand (LWS) can be effectively dispersed in matrix and progressively release water for internal curing after concrete setting. Weiss et al.[12] observed that adequate addition of LWS can increase the mechanical strength and reduce the autogenous shrinkage of concrete. Meng and Khayat[13] investigated the properties of UHPC prepared with different ratios of normalweight river sand (NS) replaced by LWS, by mass (LWS/NS), from 0 to 75%. It was found that the autogenous shrinkage decreased with the increase of LWS content.[13] The mechanical properties including compressive strength, flexural properties, and modulus of elasticity increased as the LWS/NS was increased from 0 to 25%, but decreased as the LWS/NS was increased from 25 to 75%.[13] In other words, 25% is the optimum LWS replacement ratio that can be adopted in UHPC to secure the highest mechanical properties and relatively low autogenous shrinkage.[13]

In this study, LWS partially substitutes the NS at a ratio of up to 25% to prepare UHPC mixtures. A statistical fractional factorial design approach was employed to evaluate the influence of the primary mixture design parameters and their coupling effects on the key material properties of UHPC. The investigated mixture design parameters included the *w*/*cm*, LWS/NS, and cementitious materials-to-sand ratio (*cm*/*s*). The investigated material properties included the flow time, plastic viscosity, high-range water reducer (HRWR) demand, compressive strength, and autogenous shrinkage. The formulas of the material properties were derived by regression analysis considering mixture design parameters and used for optimizing UHPC mixtures.

The Appendix to this paper is available at **www.concrete.org/publications** in PDF format, appended to the online version of the published paper. It is also available in hard copy from ACI headquarters for a fee equal to the cost of reproduction plus handling at the time of the request.

ACI Materials Journal, V. 115, No. 1, January 2018.
MS No. M-2017-099.R1, doi: 10.14359/51700995, was received April 6, 2017, and reviewed under Institute publication policies.

RESEARCH SIGNIFICANCE

This study is a significant development based on the authors' previous studies.[3,13] In the previous studies, by using 25% of LWS, the mechanical properties of the cost-effective UHPC were significantly improved with reduced shrinkage.[13] However, other critical mixture design parameters (that is, *w*/*cm* and *cm*/*s*) and their coupling effects were not investigated. In this study, the most significant parameters that influence the properties of UHPC are identified. Knowledge gained from this study can be used to develop mixture design guidelines and internal curing provisions to promote a wider acceptance of LWS as a key component for UHPC.

EXPERIMENTAL INVESTIGATION

Raw materials

ASTM Type III portland cement was used. A locally available Class C fly ash and silica fume were used as supplementary cementitious materials for partial replacement of the cement. The Blaine fineness values of the cement and fly ash were 560 and 465 m^2/kg (336,000 and 279,000 $in.^2$/lb), respectively. The silica fume particles had a mean diameter (d_{50}) of 0.15 µm (6×10^{-6} in.) and a SiO_2 content of 96%. The specific surface area of silica fume was 18,200 m^2/kg (10,865,600 $in.^2$/lb), which was determined using the Brunauer, Emmet, and Teller (BET) method. The specific gravities of the cement, fly ash, and silica fume were 3.14, 2.70, and 2.20 g/cm^3 (7.60, 6.53, and 5.32 lb/qt), respectively. Well-graded river sand, fine sand, and LWS were employed, and their properties are listed in Table 1.

Micro steel fibers measuring 0.2 mm (0.008 in.) in diameter and 13 mm (0.512 in.) in length were used at 2% of the volume of UHPC. The tensile strength and modulus of elasticity of the fibers are 1.9 and 203 GPa (285 and 30,450 ksi), respectively. A polycarboxylate-based HRWR with a solid mass content of 23% and a specific gravity of 1.05 was used to improve the flowability of UHPC. A de-air-entraining admixture with a specific gravity of 0.97 was employed to decrease the air content in the UHPC mixtures.

The moisture content of bulk LWS was measured in accordance with ASTM C128 to determine the water demand for reaching the saturated surface-dry condition (SSD). Enough water was introduced accordingly to the bulk LWS in a mixer. The LWS was then homogenized thoroughly and placed in sealed plastic bags for at least 24 hours before batching to ensure the SSD condition of the LWS. The relative desorption of the LWS was determined to be 96.4% using the centrifuge method in accordance with ASTM C1761.[14] In addition, Henkensiefken[15] reported that 96.0% of water in this type of LWS was lost at a 92.0% relative humidity (RH), implying that water can be effectively transported from the LWS to cement paste at a high RH for internal curing.

Table 1—Properties of three types of sand

Properties	LWS	River sand	Fine sand
Maximum particle size, mm (in.)	4.75 (0.2)	4.75 (0.2)	2.00 (0.08)
Specific gravity	1.78	2.64	2.64
Absorption value, %	15.6	0.14	0.06
Fineness modulus	2.94	2.71	1.74

Mixture design

A total of 16 UHPC mixtures were prepared and tested. The investigated UHPC had a fixed binder composition consisting of 55% portland cement, 40% fly ash, and 5% silica fume by volume, which was optimized in the authors' previous study.[3] The volume ratio of fine sand to river sand was fixed at 30% and 70%, by volume, respectively. The 2% micro steel fibers, by volume, were fixed for all investi-

Table 2—Details of experimental program

Mixture No.	Coded value			Type	Absolute value		
	w/*cm*	LWS/NS	*cm*/*s*		*w*/*cm*	LWS/NS	*cm*/*s*
1	–1	–1	1	Fractional factorial points	0.17	0	1.20
2	–1	1	–1		0.17	0.250	0.80
3	–1	–1	–1		0.17	0	0.80
4	–1	1	1		0.17	0.250	1.20
5	1	–1	–1		0.23	0	0.80
6	1	1	1		0.23	0.250	1.20
7	1	–1	1		0.23	0	1.20
8	1	1	–1		0.23	0.250	0.80
9	0	0	0	Central points	0.20	0.125	1.00
10	0	0	0		0.20	0.125	1.00
11	0	0	0		0.20	0.125	1.00
12	0	0	0		0.20	0.125	1.00
13	–1/3	1	–1/3	Validation points	0.19	0.250	0.93
14	1/3	1/3	–1		0.21	0.167	0.80
15	–1/3	–1/3	1		0.19	0.083	1.20
16	1/3	–1	1/3		0.21	0	1.07

Table 3—Absolute and coded values of modeled parameters (from –1 to +1)

Coded value	Absolute value		
	w/*cm*	LWS/NS	*cm*/*s*
–1	0.17	0	0.80
0	0.20	0.125	1.00
+1	0.23	0.250	1.20

gated mixtures to achieve adequate tensile/flexural strength and ductility,[3] as required by ACI 239.[16] A statistical fractional factorial design approach was used to formulate the 16 UHPC mixtures shown in Table 2 for evaluating the three primary proportioning parameters, which are the *w*/*cm*, LWS/NS, and *cm*/*s*. The LWS/NS was calculated by volume ratio of the lightweight sand to the sum of lightweight sand and the river sand. Each parameter was evaluated at two distinct values, coded as –1 and +1, which correspond to the minimum and the maximum levels, respectively. Mixtures 1 to 8 were investigated to establish a 2^3 factorial design for the three parameters. Mixtures 9 to 12 were prepared to represent the center points in the design for obtaining a measure of experimental error. Mixtures 13 to 16 were prepared for validating the statistical models. In accordance with ASTM C230, the initial mini-slump flow of all mixtures was regulated to 280 ± 10 mm (11.2 ± 0.4 in.) by adjusting the HRWR dosage. The dosage of de-air-entraining admixture was fixed at 0.8% for all of the 16 mixtures. The mixture proportions of Mixtures 9 to 12 are reported for example: cement = 663 kg/m^3 (390 lb/yd^3), silica fume = 42 kg/m^3 (25 lb/yd^3), fly ash = 367 kg/m^3 (216 lb/yd^3), lightweight sand = 60 kg/m^3 (35 lb/yd^3), river sand = 615 kg/m^3 (362 lb/yd^3), fine sand = 308 kg/m^3 (181 lb/yd^3), HRWR = 12 kg/m^3 (7 lb/yd^3), total water = 171 kg/m^3 (100.5 lb/yd^3), air-detraining admixture = 8.5 kg/m^3 (5 lb/yd^3), steel fiber = 156 kg/m^3 (91.8 lb/yd^3).

The absolute values corresponding to the coded values of the primary variables are presented in Table 3. The coded values were calculated as the difference between the absolute values and the values corresponding to the centerpoints divided by half the spread between the maximum and minimum values, as shown in Eq. (1)

$$\begin{aligned}\text{Coded } w/cm &= (\text{absolute } w/cm \quad 0.20)/0.03\\ \text{Coded LWS/NS} &= (\text{absolute LWS/NS} \quad 0.125)/0.125\\ \text{Coded } cm/s &= (\text{absolute } cm/s \quad 1)/0.2\end{aligned} \tag{1}$$

Mixing, casting, and curing

All mixtures were prepared using a 19 L (20 qt) mortar mixer. The mixing procedure consisted of: 1) homogenizing sand at a speed of 60 rpm for 60 seconds; 2) introducing the cement, fly ash, and silica fume, and mixing at 60 rpm for 2 minutes; 3) introducing 90% water and 90% HRWR, and mixing at 120 rpm for 3 minutes; 4) adding the rest of water and HRWR, and mixing at 120 rpm for 6 minutes; 5) gradually adding fibers within 1 minute at a mixing speed of 60 rpm; and finally 6) mixing the mixture at 120 rpm for another 2 minutes before concrete casting. The mixing was performed at room temperature (23 ± 1ºC [73.4 ± 1.8ºF]). All specimens were cast in one lift without performing any mechanical consolidation.

After casting, the specimens were immediately covered with wet burlap and a plastic sheet. The specimens were demolded after 24 hours and then cured in lime-saturated water at room temperature until the time of testing.

Fresh properties

The specific gravity and air content of the mixtures were measured in accordance with ASTM C138 and ASTM C173,[14] respectively. The HRWR demand (percentage of active portion of HRWR to cementitious materials, by mass, was adjusted to secure a mini-slump flow of 280 ± 10 mm (11.2 ± 0.4 in.). The flow time was measured using a mini V-funnel according to EFNARC recommendations.[17]

Rheological properties

A viscometer was employed to test the dynamic yield stress τ_0 and plastic viscosity μ_p of the UHPC mixtures. The viscometer is a wide gap concentric cylinder rheometer with an inner cylinder radius of 100 mm (4 in.) and an outer cylinder radius of 145 mm (5.8 in.). The measurements were started 10 minutes after water was added in the mixer. The test started with a pre-shear period of 25 seconds at a rotational velocity of 0.5 rps, followed by a stepwise decrease in rotational velocity from 0.5 to 0.025 rps within ten 5-second steps. The torque and velocity were recorded by the rheometer. The yield stress and plastic viscosity were calculated using the Bingham fluid model as shown in Eq. (2)[18]

$$\tau = \tau_0 + \mu_p \dot{\gamma} \tag{2}$$

Autogenous shrinkage

Autogenous shrinkage was evaluated in accordance with ASTM C1698. Three specimens were cast in standard corrugated plastic tubes for autogenous shrinkage measurement of each UHPC mixture. The tubes for the autogenous shrinkage testing were 420 mm (16.5 in.) long. The diameter of the tubes was 30 mm (1.2 in.) at the ridge and 25 mm (1.0 in.) at the groove. The specimens were stored at room temperature (23 ± 1°C [73.4 ± 1.8ºF]) and a relative humidity of 50% ± 2%. Shrinkage measurements were performed at final setting and 12 hours after the final setting, and then on daily basis for the first week and on weekly basis until the age of 28 days.

Compressive strength

For all investigated UHPC specimens, compressive strength at 1, 3, 7, 28, and 91 days was tested using 50 mm (2 in.) cubes in accordance with ASTM C109. The cube specimens were tested using a load frame (load capacity: 250 kN [55 kip]) at a loading rate of 1.8 kN/min (0.4 kip/min).

EXPERIMENTAL RESULTS AND DISCUSSIONS

Experimental results and statistical models

Table 4 summarizes the experimental results of the 16 UHPC mixtures, including the specific gravity; air content; HRWR demand; flow time; plastic viscosity; dynamic yield

Table 4—Summary of test results

Mixture No.	1	2	3	4	5	6	7	8	9	10	11	12	13	14	15	16
Fresh properties																
Specific gravity	2.52*	2.40	2.46	2.41	2.42	2.40	2.49	2.36†	2.41	2.40	2.39	2.42	2.35	2.37	2.49	2.38
Air content, %	2.5*	2.5	2.0	2.0	2.5	2.5	2.5	2.5	1.5	1.0†	1.0	1.5	2.0	2.5	2.0	1.5
HRWR demand, %	0.9	1.0*	1.0	0.9	0.7	0.6†	0.6	0.7	0.7	0.7	0.7	0.8	0.8	0.8	0.8	0.7
Flow time, seconds	30.2*	26.1	29.6	28.2	8.5	7.7†	12.3	8.1	18.1	17.6	17.4	17.2	21.2	15.1	23.3	17.2
Mini-slump flow, mm	270	270	290	270	290	290	280	280	290	270	270	270	280	290	270	280
Rheological properties																
Plastic viscosity, Pa·s	28.8*	21.6	26.6	23.2	4.4	3.9†	7.2	4.1	16.1	11.6	12.3	15.4	20.5	14.6	25.5	17.6
Yield stress, Pa	6.5	9.6	3.9	4.6	16.1	13.0	6.5	19.1	14.3	19	10.4	15.2	4.2	6.0	15.8	14.4
Autogenous shrinkage, μm/m																
1 day	502*	100	226	165	168	94	388	23†	223	206	213	241	100	95	336	350
3 day	693*	135	345	310	280	152	520	34†	349	338	353	323	168	176	425	462
7 day	831*	187	558	436	388	240	627	47†	462	421	432	444	210	218	592	600
28 day	893*	200	609	440	406	260	676	72†	492	456	465	479	226	233	611	632
Compressive strength, MPa																
1 day	59*	46	59	48	42	44	38†	47	50	53	50	52	50	47	51	42
3 day	86*	70	83	65†	79	62	78	80	73	78	69	75	80	69	77	80
7 day	124	126	115	132*	103†	121	111	119	116	114	118	115	121	121	121	118
28 day	145	148	135	160*	123†	140	132	136	144	142	140	141	143	136	138	139
91 day	151	156	139	170*	125†	147	135	141	156	150	150	152	152	146	145	146

*Maximal value.

†Minimal value.

Notes: 1 μm/m = 1 × 10^{-6} in./in.; 1 MPa = 0.15 ksi; 1 Pa·s = 1.5 ×.10^{-4} psi·s; 1 Pa = 1.5 × 10^{-4} psi; 1 mm = 0.04 in.

stress; mini-slump flow; autogenous shrinkage at 1, 3, 7, and 28 days; and compressive strengths at 1, 3, 7, 28, and 91 days.

Statistical analysis of the effects of the LWS/NS, *w*/*cm*, and *cm*/*s* on UHPC properties was performed using the Design-Expert® software.[19] The investigated properties were formulated as functions of the investigated mixture proportioning parameters by performing multiple linear regression analyses using the least-squares method. The derived statistical models are listed in Table 5. These statistical models were established in three steps:

1. For each material property, a multiple linear regression analysis was performed to establish the mathematical equations, taking the three mixture design parameters (*w*/*cm*, LWS/NS, and *cm*/*s*) and their products as input variables.

2. After the mathematical equation of each material property is generated, the probability value (*p*-value) is examined for each variable to ensure the variable has statistically significant influence on the material property. If the *p*-value of a variable is larger than 0.05, the variable is identified as a statistically insignificant variable, and thus removed from the equation. This step is repeated until all insignificant variables are removed from the statistical equations.

3. All influencing parameters are expressed using the coded values (–1 to +1). In the derived equations in Table 5, the variables are listed in a descending order in terms of the degree of significance, which is represented by the coefficient in front of the variable. The positive or negative sign of each coefficient manifests the property increases or decreases with the corresponding variable.

The product of multiple influencing parameters—for instance, (*w*/*cm*) × (*cm*/*s*)—suggests the coupling effect of the mixture design parameters. The coefficients of determination R^2 of the derived models ranged from 0.85 to 0.98, indicating adequate agreement between the test data and the statistical models. The relative errors were determined using mixtures corresponding to the central point of the experimental domain.

Fresh properties

As shown in Table 4, the values of specific gravity of the mixtures in fresh condition slightly decreased with the increasing content of lightweight sand. The variation range was 2.39 to 2.52, which is relatively small and insignificant. The air content was in the range of 1 to 2.5%; the larger entrapped air content was associated with mixtures of greater viscosity. The HRWR demand (mass ratio of active solid HRWR to cementitious materials) for achieving the targeted mini-slump spread value of 280 ± 10 mm (11.2 ± 0.4 in.) was in a range of 0.5 to 1.0%. A lower HRWR indicates better flowability prior to the addition of HRWR. The mini V-funnel flow time of the investigated mixtures was in a range of 7.7 to 30.2 seconds.

As indicated in Table 5, the *w*/*cm* has the most significant effect on the HRWR demand. The *w*/*cm* also has the highest impact on flow time, which far exceeds the effects

Table 5—Derived statistical models for UHPC properties (based on coded value)

	Derived equations	R^2	*p*-value
	HRWR demand, %		
	0.78 to 0.16 *w*/*cm* – 0.05 *cm*/*s*	0.92	<0.0001
	Flow time, seconds		
	18.42 to 9.69 *w*/*cm* – 1.31 LWS/NS	0.98	<0.0001
	Plastic viscosity, Pa·s		
	14.60 to 10.08 *w*/*cm* – 1.78 LWS/NS	0.96	<0.0001
	Autogenous shrinkage, μm/m		
1 day	210.92 – 112.75 LWS/NS + 81.25 *cm*/*s* – 46.25 *w*/*cm* – 45.00 (LWS/NS) × (*cm*/*s*)	0.94	0.0002
7 day	413.58 – 190.50 LWS/NS + 113.00 *cm*/*s* – 82.50 *w*/*cm*	0.95	<0.0001
28 day	442.75 – 205.88 LWS/NS + 115.13 *cm*/*s* – 88.63 *w*/*cm*	0.95	<0.0001
	Compressive strength, MPa		
1 day	49.00 – 5.13 w/cm + 4.38 (*w*/*cm*) × (LWS/NS)	0.85	0.0003
3 day	74.83 – 6.13 LWS/NS – 3.12(*cm*/*s*) × (LWS/NS) – 2.63 *cm*/*s* + 2.38(*w*/*cm*) × (LWS/NS) – 2.12(*w*/*cm*) × (*cm*/*s*)	0.90	0.0075
7 day	117.83 + 5.62 LWS/NS – 5.38 *w*/*cm* + 3.12 *cm*/*s*	0.91	0.0002
28 day	140.50 – 7.13 *w*/*cm* + 6.12 LWS/NS + 4.37 *cm*/*s*	0.95	<0.0001
91 day	147.67 – 8.50 *w*/*cm* + 8.00 LWS/NS + 5.25 *cm*/*s*	0.90	0.0003

Notes: 1 μm/m = 1 × 10^{-6} in./in.; 1 MPa = 0.15 ksi; 1 Pa·s = 1.5 × 10^{-4} psi·s.

of the LWS/NS and *cm*/*s* on the flow time. Increasing the *w*/*cm* can reduce the flow time, thus enhancing the filling capacity of the UHPC. Therefore, it is critical to balance the mechanical properties and fresh properties by adjusting *w*/*cm* of the UHPC.

Rheological properties

Reducing plastic viscosity μ_p is essential to facilitate placement and enhance the filling ability of self-consolidating materials, such as UHPC. The derived statistical models in Table 5 indicate that the *w*/*cm* has the most significant effect on μ_p and t_f. The influences of LWS/NS on μ_p and t_f can be considered as secondary effects compared with *w*/*cm*. The decrease of μ_p and t_f by adding LWS can be attributed to the relatively round geometry of LWS compared with NS.

Autogenous shrinkage

Figure 1 shows the autogenous shrinkage of the investigated UHPC mixtures made with different combinations of *w*/*cm*-LWS/NS-*cm*/*s* in the first 28 days. The autogenous shrinkage of the 0.17-0-1.2 mixture (*w*/*cm*-LWS/NS-*cm*/*s*: 0.17-0-1.2) is shown to increase dramatically after final setting. The autogenous shrinkage reached approximately 500 μm/m (500 × 10^{-6} in./in.) at 1 day and 800 μm/m at 28 days. The autogenous shrinkage was substantially reduced when the *w*/*cm* and LWS/NS were increased and/or the *cm*/*s* was reduced. For instance, the 28-day autogenous shrinkage of the 0.23-0.25-0.8 mixture was 50 μm/m (50 × 10^{-6} in./in.), which is 90% lower than that of the 0.17-0-1.2 mixture. As the LWS/NS increased from 0 to 0.25, the 28-day autogenous shrinkage decreased by 70% compared with the 0.17-0-0.8 and 0.17-0.25-0.8 mixtures, by 50% for the 0.17-0-1.2 and 0.17-0.25-1.2 mixtures, by 70% for the 0.23-0-0.8 and 0.23-0.25-0.8 mixtures, and by 75% for the 0.23-0-1.2 and 0.23-0.25-1.2 mixtures. This indicates that the addition of LWS can significantly reduce autogenous shrinkage. Due to internal curing effect from the LWS, self-desiccation is reduced, resulting in proportionally lower self-induced stresses.[20,21]

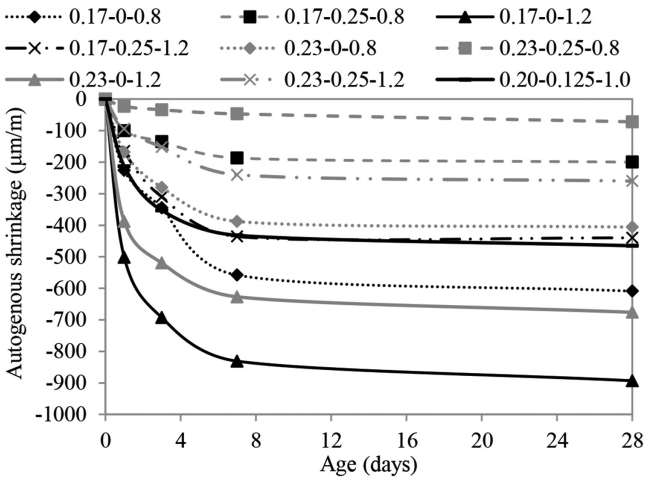

Fig. 1—Autogenous shrinkage of UHPC mixtures with different w/cm-*LWS/NS*-cm/s *combinations. (Note: 1 μm/m = 1 × 10^{-6} in./in.)*

Table 5 indicates that the LWS/NS has the most significant influence on the 1-, 7-, and 28-day autogenous shrinkages of the UHPC mixtures, followed by the *cm*/*s*. The *w*/*cm* demonstrates more impact on the 28-day autogenous shrinkage than that on the 1-day autogenous shrinkage. Figures 2(a) and (b) respectively show the contour diagrams of the 1- and 28-day autogenous shrinkages of the UHPC mixtures with 0.20 *w*/*cm*. The tradeoff between the *cm*/*s* and the LWS/NS is illustrated. The 1- and 28-day autogenous shrinkage results decreased with the LWS/NS and

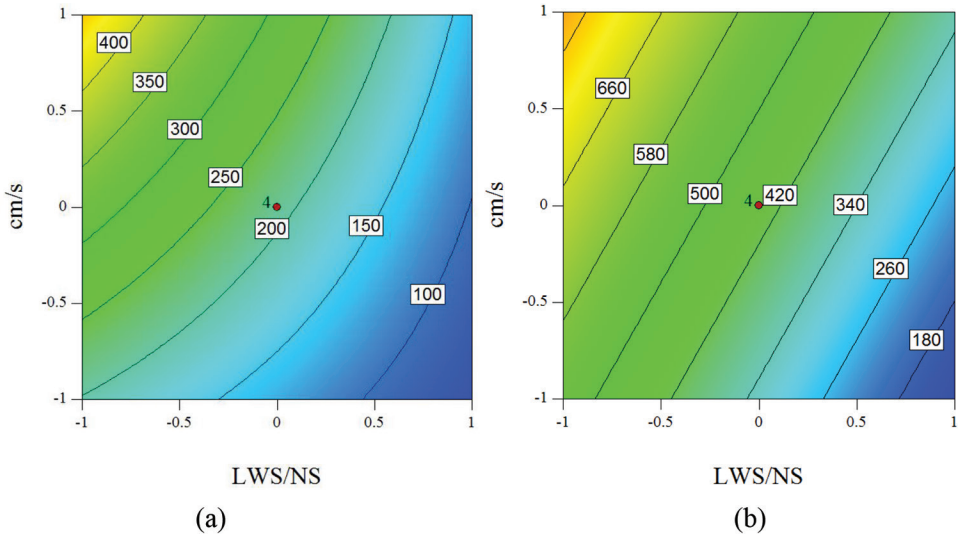

*Fig. 2—cm/s-LWS/NS (coded value) contour diagrams of autogenous shrinkage at: (a) 1 day, and (b) 28 days (*w/cm *coded as 0). (Note: Units are in μm/m; 1 μm/m = 1 × 10^{-6} in./in.)*

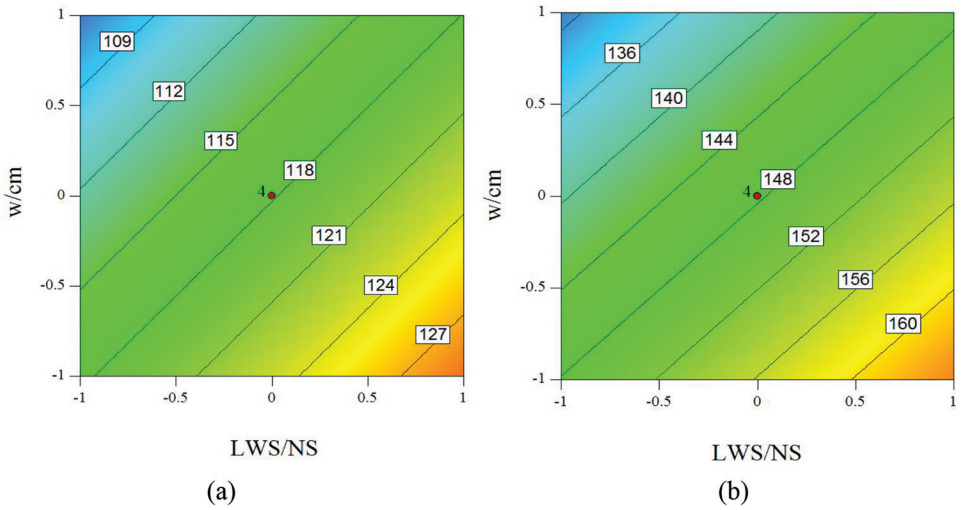

*Fig. 3—*w/cm*-LWS/NS (coded value) contour diagrams of compressive strength at: (a) 7 days; and (b) 91 days (*cm/s *coded as 0). (Note: Units are in MPa; 1 MPa = 0.145 ksi.)*

increased with the *cm*/*s*. Figure 2(a) shows that as the LWS/NS was increased from 0 to 0.25, the 1-day autogenous shrinkage was reduced by approximately 150 μm/m (150 × 10^{-6} in./in.), and as the *cm*/*s* was reduced from 1.20 to 0.80, the 1-day autogenous shrinkage decreased by approximately 360 μm/m (360 × 10^{-6} in./in.). Figure 2(b) shows that, as the LWS/NS was increased from 0 to 0.25, the 28-day autogenous shrinkage was reduced by approximately 400 μm/m (400 × 10^{-6} in./in.), and as the *cm*/*s* was reduced from 1.20 to 0.80, the 28-day autogenous shrinkage was reduced by 380 μm/m (380 × 10^{-6} in./in.).

Compressive strength

For the compressive strengths at 1 and 3 days, the LWS/NS demonstrated negative effects (Table 5), meaning the use of LWS reduced the compressive strength at early ages. However, the LWS/NS demonstrated positive effects on the compressive strength at 7, 28, and 91 days. The coefficient of the LWS/NS increased monotonically from +5.62 at 7 days to +8.00 at 91 days, indicating the use of LWS enhanced the compressive strength of the UHPC mixtures and the enhancement becomes more significant at latter ages. Figures 3(a) and (b) show the contour diagrams of the 7- and 91-day compressive strengths of the UHPC mixtures associated with the LWS/NS and *w*/*cm*, with the *cm*/*s* fixed at 1.0. The 7- and 91-day compressive strengths increased with the LWS/NS and decreased with the *w*/*cm*. With a *w*/*cm* of 0.17, as the LWS/NS was increased from 0 to 0.25, the 7- and 91-day compressive strengths were increased by approximately 10% and 15%, respectively.

With the addition of LWS, the compressive strength was significantly increased. At early ages, the porous LWS and water released from the pre-saturated LWS increased the porosity of the hydraulic UHPC system, thus reducing the compressive strength. However, at later ages, the released water promoted the hydration reactions of cementitious materials, thus increasing compressive strength of UHPC.[22] The released water during the curing process help sustain a relatively high humidity in UHPC for extended periods,

Table 6—Mean values and relative errors of central points at 95% confidence level

Property	Age	Mean	Error	Relative error, %
HRWR demand, %	—	0.74	0.03	5.8
Flow time	—	17.6	0.8	4.8
Plastic viscosity, Pa·s (psi·s)	—	13.9 (20.16 × 10^{-4})	0.8	5.4
Autogenous shrinkage, μm/m (in./in.)	1	220.8 (220.8 × 10^{-6})	9.8	4.5
	7	439.8 (439.8 × 10^{-6})	26.2	6.0
	28	473.0 (473.0 × 10^{-6})	30.3	6.4
Compressive strength, MPa (ksi)	1	51.3 (7.7)	2.3	4.4
	3	73.7 (11.1)	1.1	1.5
	7	115.8 (17.4)	2	1.8
	28	141.8 (21.3)	1.3	0.9
	91	152 (22.8)	4.3	2.9

which is necessary for continued hydrations of Belite and pozzolanic reactions of fly ash and silica fume.[23]

The *w*/*cm* has a negative effect on the compressive strength, and the negative effect becomes magnified at the latter ages. Significant positive coupling effects of the *w*/*cm* and LWS/NS on the 1- and 3-day compressive strength are demonstrated, indicating that the negative effect of *w*/*cm* was suppressed by using LWS, which results in a greater level of hydration. The *cm*/*s* has negative effects on the compressive strength at 3 days, but positive effects at a latter age. At early age, the strength of cementitious materials matrix was lower than that of sand due to the relatively low degree of hydration; therefore, increasing the *cm*/*s* reduced the compressive strength. However, at the later ages, the matrix gained substantially high strength due to the increased degree of hydration. Thus, increasing the *cm*/*s* increased the compressive strength.

Evaluation and validation of statistical models

The four mixtures (Mixtures No. 9 through 12) corresponding to central points were used to evaluate the error (that is, the discrepancy between the test data and predicted values from the statistical models) at 95% confidence level. These values are listed in Table 6. The relative error is defined as the ratio of the error to the mean value.

The predicted and measured values of the HRWR demand, flow time, autogenous shrinkage, and compressive strength at different ages of 16 mixtures (Mixtures No. 1 through 16) are compared in Fig. 4(a) to (d). In each figure, the solid line represents the 1:1 line; the two dashed lines correspond to the upper and lower limits, respectively, of the material property at 95% confidence level. Any data point above the solid line represents an overestimated value of the property, and any data point below the solid line represents an underestimated value. The majority of the data points are shown to fall into the range between the dashed lines, indicating that the proposed models allow adequate prediction of the material properties.

Optimization of UHPC mixtures

The validated statistical models were employed to optimize the UHPC mixtures using a numerical optimization technique with desirability functions[24,25] according to the responses of the materials properties. Table 7 lists the optimization criteria and seven material properties that were taken into account for the evaluation of the overall performance of the various UHPC mixtures.[24] A goal was set as either minimal or maximal for each materials property according to the desired response. For the HRWR demand, plastic viscosity, and autogenous shrinkage, a minimum goal was set. On the other hand, in the case of compressive strength, maximum goal was desired.

Because the optimization was based on the formulated statistical models, which were valid within a specific range of each proportioning variable, a lower and an upper limit should be set for each material property. The lower and upper limits of any material property correspond to minimal and maximal experimental results of that property, respectively. These values are reported in Table 4. Any predicate response of material property that lies outside of the lower and upper limits was not taken into consideration in the mixture optimization. The weight factors of the lower and upper limits were taken as 1. The significance of each material property was empirically valued from 1 to 5. A larger significance value represents a more important material property of UHPC.

According to the goals of the material properties, a desirability index d_i ranging from 0 to 1 was introduced for each of the seven material properties.[24] For a material property with a goal of minimal value, the desirability is linearly changed from 1 at the lower limit to 0 at the upper limit. Similarly, for a material property with a goal of maximal value, the desirability is linearly changed from 1 at the upper limit to 0 at the lower limit.[24] A higher desirability value indicates higher performance level. With the seven desirability indexes (d_1 to d_7), an overall desirability D was defined to represent the overall performance of each UHPC mixture, as indicated in Eq. (3)[26]

$$D = \left(\prod_{i=1}^{7} d_i^{r_i} \right)^{\frac{1}{\sum r_i}} \tag{3}$$

where r_i represents the significance value; and i represents the number of material properties (Table 7).

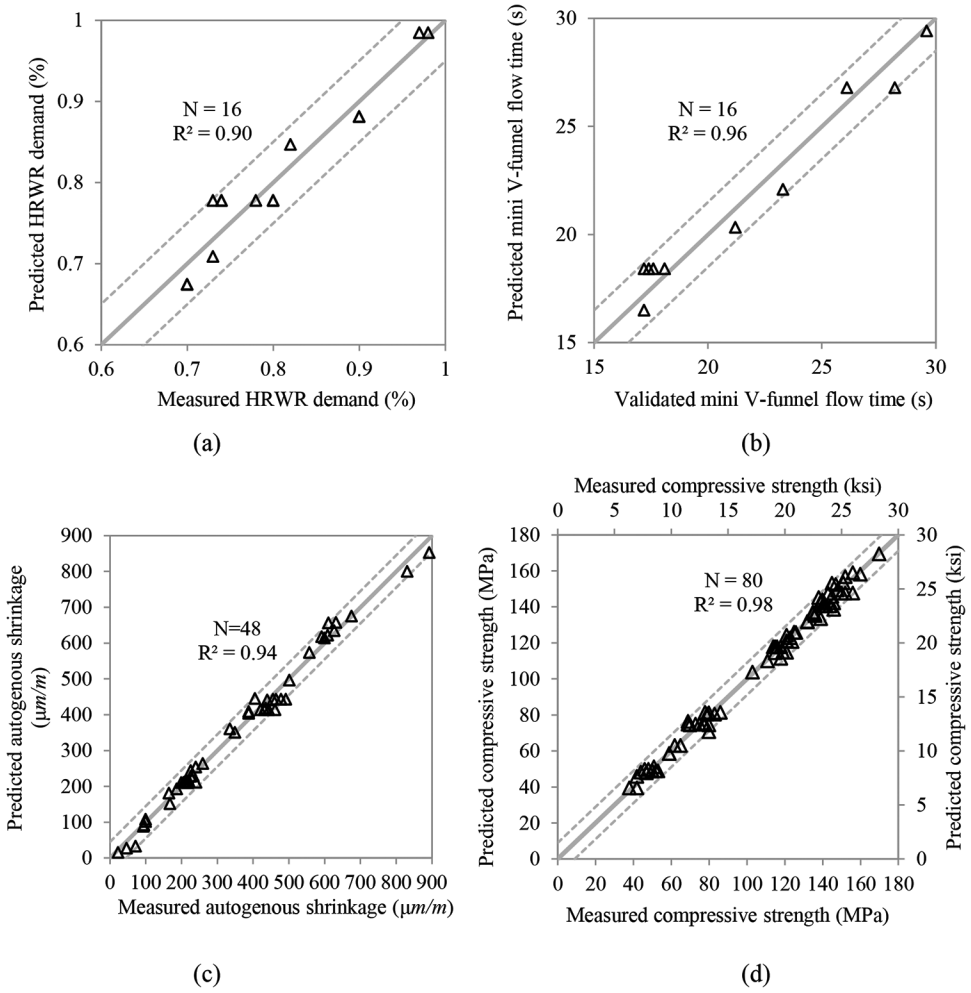

Fig. 4—Comparison between predicted and measured values for: (a) HRWR demand; (b) mini V-funnel flow time; (c) autogenous shrinkage at 1, 7, and 28 days; and (d) compressive strength at 1, 3, 7, 28, and 91 days. "N" denotes number of data points. (Note: 1 μm/m = 1 × 10^{-6} in./in.)

Table 7—Criteria for optimizing UHPC mixtures

No.	Material property	Goal	Lower limit	Upper limit	Significance
1	HRWR demand, %	Minimal	0.6	1.0	5
2	Plastic viscosity, Pa·s (psi·s)	Minimal	3.9 (5.7 × 10^{-4})	28.8 (41.8 × 10^{-4})	5
3	1-day autogenous shrinkage, μm/m (in./in.)	Minimal	23 (23 × 10^{-6})	502 (509 × 10^{-6})	5
4	28-day autogenous shrinkage, μm/m (in./in.)	Minimal	72 (72 × 10^{-6})	893 (893 × 10^{-6})	5
5	1-day compressive strength, MPa (ksi)	Maximal	38 (5.7)	59 (8.9)	1
6	28-day compressive strength, MPa (ksi)	Maximal	123 (18.5)	160 (24)	3
7	91-day compressive strength, MPa (ksi)	Maximal	125 (18.8)	170 (25.5)	5

Table 8—Top candidates of optimized UHPC mixtures

Rank	LWS/NS	*cm*/*s*	*w*/*cm*	Desirability
1	0.25	1.20	0.23	0.795
2	0.25	1.10	0.23	0.783
3	0.25	1.20	0.21	0.762
4	0.25	1.00	0.23	0.758
5	0.25	0.90	0.22	0.754
6	0.21	1.20	0.22	0.731

Within the ranges of mixture proportioning variables (0.17 to 0.23 for the *w*/*cm*, 0.8 to 1.2 for the *cm*/*s*, and 0 to 0.25 for the LWS/NS), *w*/*cm*, *cm*/*s*, and LWS/NS were changed with a step size of 0.01, 0.1, and 0.01, respectively. The overall desirability values of a total of 910 UHPC mixtures were calculated and compared. The highest overall desirability value is 0.795. Table 8 lists the top six candidate mixtures in terms of the value of the overall desirability. For the six candidates, the LWS/NS corresponds to 0.25, the *w*/*cm* is in the range of 0.21 to 0.23, and the *cm*/*s* is various between 0.90 and 1.20. In particular, the 0.23-0.25-1.2 mixture

(*w*/*cm* = 0.23, LWS/NS = 0.25, *cm*/*s* = 1.2) was ranked the best mixture (No. 1). The properties of the 0.23-0.25-1.2 mixture were tested: a HRWR demand was 0.6%; the plastic viscosity was 3.9 Pa·s ($5.91.5 \times 10^{-4}$ psi·s); the 1-day autogenous shrinkage was 94 μm/m (94×10^{-6} in./in.); the 28-day autogenous shrinkage was 260 μm/m (260×10^{-6} in./in.); the 1-, 28-, and 91-day compressive strengths were 44, 140, and 147 MPa (6.6, 21, and 22 ksi), respectively.

CONCLUSIONS

Based on the aforementioned investigations, the following conclusions can be drawn:

1. By partially replacing river sand with lightweight sand, UHPC mixtures can be produced to achieve improved flowability, plastic viscosity, compressive strength, and autogenous shrinkage properties. As the LWS/NS was increased from 0 to 25%, the compressive strength at 91 days was increased by up to 15%, and the autogenous shrinkage at 28 days was reduced by up to 75%.

2. Among the *w*/*cm*, LWS/NS, and *cm*/*s*, the *w*/*cm* was the parameter that had the most significant influence on the compressive strength at the ages of 7 days or later, followed by the LWS/NS and then the *cm*/*s*. The compressive strength decreased with the *w*/*cm* and increased with the LWS/NS and *cm*/*s*. The coupling effects of the three parameters on compressive strength were significant in the first 3 days and then become insignificant after 7 days.

3. The LWS/NS was the parameter that had the most significant influence on autogenous shrinkage at 28 days, followed by the *cm*/*s* and then the *w*/*cm*. The autogenous shrinkage decreased with the increase of LWS/NS and *cm*/*s*, and increased with the increase of *w*/*cm*. The coupling effects of the three parameters on autogenous shrinkage were insignificant at 7 and 28 days.

4. When the *w*/*cm* was 0.17 and the *cm*/*s* was 1.2, increasing the LWS/NS from 0 to 25% reduced the 28-day autogenous shrinkage from 890 to 440 μm/m (890 to 440 × 10^{-6} in./in.), and increased the 91-day compressive strength from 150 to 170 MPa (22.5 to 25.5 ksi). When the *w*/*cm* was 0.23 and the *cm*/*s* was 1.2, increasing the LWS/NS from 0 to 25% reduced the 28-day autogenous shrinkage from 680 to 260 μm/m (680 to 260 × 10^{-6} in./in.), and increased the 91-day compressive strength from 135 to 145 MPa (20.3 to 21.8 ksi).

5. The developed statistical models allow prediction of the material properties of the UHPC mixtures with relative errors less than 10%. Using the validated formulas, UHPC mixtures can be optimized in terms of the desirability of material properties, given the optimization criteria for different applications. With the objective to minimize autogenous shrinkage and maximize the compressive strengths, an optimized UHPC mixture 0.23-0.25-1.2 (*w*/*cm*-LWS/NS-*cm*/*s*) was recommended.

AUTHOR BIOS

ACI member **Weina Meng** *is a Postdoctoral Fellow in civil engineering at Missouri University of Science and Technology, Rolla, MO. Her research interests include design, development, and applications of ultra-high-performance concrete, nanocomposites, and smart materials.*

V. A. Samaranayake *is a Professor of mathematics and statistics at Missouri University of Science and Technology. His research interests include time series analysis and forecasting; reliability analysis; biostatistics; and statistical applications in economics, engineering, and the social sciences.*

Kamal H. Khayat, *FACI, is the Vernon and Maralee Jones Chair Professor in Civil Engineering at Missouri University of Science and Technology. He received his BS, MS, and PhD from University of California, Berkeley, Berkeley, CA. He is past Chair of ACI Committee 237, Self-Consolidating Concrete, from 2009 to 2015. He is a member of ACI Committees 234, Silica Fume in Concrete; 236, Material Science of Concrete; 238, Workability of Fresh Concrete; 347, Formwork for Concrete; and 552, Cementitious Grouting.*

ACKNOWLEDGMENTS

This study was funded by RE-CAST Tier – 1 University Transportation Center at Missouri S&T (Grant No. DTRT13-G-UTC45) and the Energy Consortium Research Center at Missouri S&T (Grant No. SMR-1406-09).

REFERENCES

1. Graybeal, B., "Material Property Characterization of Ultra-High Performance Concrete," *FHWA-HRT-06-103*, Federal Highway Administration, U.S. Department of Transportation, Washington, DC, 2006.

2. Habert, G.; Denarié, E.; Šajna, A.; and Rossi, P., "Lowering the Global Warming Impact of Bridge Rehabilitations by Using Ultra High Performance Fibre Reinforced Concretes," *Cement and Concrete Composites*, V. 38, 2013, pp. 1-11. doi: 10.1016/j.cemconcomp.2012.11.008

3. Meng, W.; Valipour, M.; and Khayat, K., "Optimization and Performance of Cost-Effective Ultra-High Performance Concrete," *Materials and Structures*, V. 50, No. 1, 2017. doi: 10.1617/s11527-016-0896-3

4. Meng, W., and Khayat, K. H., "Improving Flexural Performance of Ultra-High-Performance Concrete by Rheology Control of Suspending Mortar," *Composites. Part B, Engineering*, V. 117, 2017, pp. 26-34. doi: 10.1016/j.compositesb.2017.02.019

5. Meng, W., and Khayat, K. H., "Mechanical Properties of Ultra-High-Performance Concrete Enhanced with Graphite Nanoplatelets and Carbon Nanofibers," *Composites. Part B, Engineering*, V. 107, 2016, pp. 113-122. doi: 10.1016/j.compositesb.2016.09.069

6. Justs, J.; Wyrzykowski, M.; Bajare, D.; and Lura, P., "Internal Curing by Superabsorbent Polymers in Ultra-High Performance Concrete," *Cement and Concrete Research*, V. 76, 2015, pp. 82-90. doi: 10.1016/j.cemconres.2015.05.005

7. Justs, J.; Wyrzykoski, M.; Winnefeld, F.; Bajare, D.; and Lura, P., "Influence of Superabsorbent Polymers on Hydration of Cement Pastes with Low Water-to-Binder Ratio," *Journal of Thermal Analysis and Calorimetry*, V. 115, No. 1, 2014, pp. 425-432. doi: 10.1007/s10973-013-3359-x

8. Bao, Y.; Meng, W.; Chen, Y.; Chen, G.; and Khayat, K. H., "Measuring Mortar Shrinkage and Cracking by Pulse Pre-Pump Brillouin Optical Time Domain Analysis with a Single Optical Fiber," *Materials Letters*, V. 145, 2015, pp. 344-346. doi: 10.1016/j.matlet.2015.01.140

9. Bentz, D., and Weiss, J., "Internal Curing: A 2010 State-of-the-Art Review," *NISTIR 7765*, U.S. Department of Commerce, Washington, DC, 2011, 82 pp.

10. Bentz, D. P.; Lura, P.; and Roberts, J. W., "Mixture Proportioning for Internal Curing," *Concrete International*, V. 27, No. 2, Feb. 2005, pp. 35-40.

11. De la Varga, I., and Graybeal, B., "Dimensional Stability of Grout-Type Materials used as Connections between Prefabricated Concrete Elements," *Journal of Materials in Civil Engineering*, ASCE, V. 27, No. 9, 2015, p. 04014246. doi: 10.1061/(ASCE)MT.1943-5533.0001212

12. Weiss, J.; Bentz, D.; Schindler, A.; and Lura, P., "Internal Curing," *STRUCTURE*, Jan. 2012, pp. 10-14.

13. Meng, W., and Khayat, K., "Effects of Saturated Lightweight Sand Content on Key Characteristics of Ultra-High-Performance Concrete," *Cement and Concrete Research*, V. 101, 2017, pp. 46-54.

14. ASTM C1761/C1761M, "Standard Specification for Lightweight Aggregate for Internal Curing of Concrete," ASTM International, West Conshohocken, PA, 2017, 8 pp.

15. Henkensiefken, R., "Internal Curing in Cementitious Systems Made Using Saturated Lightweight Aggregate," PhD dissertation, Purdue University, West Lafayette, IN, 2008, 187 pp.

16. ACI Committee 239, "Committee in Ultra-High Performance Concrete," Minutes of Committee Meeting Oct. 2012, ACI Convention 2012, Toronto, ON, Canada.

17. EFNARC, "Specification and Guidelines for Self-Compacting Concrete," European Federation for Specialist Construction Chemicals and Concrete Systems, Norfolk, UK, English ed., 2002, 32 pp.

18. Tattersall, G. H., and Banfill, P. F. G., *The Rheology of Fresh Concrete*, Pitman, London, UK, 1983, 356 pp.

19. Vaughn, N. A., and Polnaszek, C., Design-Expert® software. Stat-Ease, Inc, Minneapolis, MN, 2007.

20. Lura, P.; van Breugel, K.; and Maruyama, I., "Effect of Curing Temperature and Type of Cement on Early-Age Shrinkage of High-Performance Concrete," *Cement and Concrete Research*, V. 31, No. 12, 2001, pp. 1867-1872. doi: 10.1016/S0008-8846(01)00601-9

21. Lura, P.; Jensen, O. M.; and van Breugel, K., "Autogenous Shrinkage in High-Performance Cement Paste: An Evaluation of Basic Mechanism," *Cement and Concrete Research*, V. 33, No. 2, 2003, pp. 223-232. doi: 10.1016/S0008-8846(02)00890-6

22. Jensen, O. M., and Hansen, P. F., "Water-Entrained Cement-Based Materials: I. Principles and Theoretical Background," *Cement and Concrete Research*, V. 31, No. 4, 2001, pp. 647-654. doi: 10.1016/S0008-8846(01)00463-X

23. Duran-Herrera, A.; Aitcin, P. C.; and Petrov, N., "Effect of Saturated Lightweight Sand Substitution on Shrinkage in 0.35 *w*/*b* Concrete," *ACI Materials Journal*, V. 104, No. 1, Jan.-Feb. 2007, pp. 48-52.

24. Montgomery, D., *Design and Analysis of Experiments*, John Wiley & Sons, Inc., New York, 2012.

25. Lotfy, A.; Hossain, K. M.; and Lachemi, M., "Application of Statistical Models in Proportioning Lightweight Self-Consolidating Concrete with Expanded Clay Aggregates," *Construction and Building Materials*, V. 65, 2014, pp. 450-469. doi: 10.1016/j.conbuildmat.2014.05.027

26. User's Manual of Design-Expert Software, Stat-Ease Inc., Minneapolis, MN, 2013.

The chemical and physical properties of the fine sand and lightweight sand are listed in Table S1. Figure S1shows the sand gradation of fine sand and lightweight sand.

Table S1. Chemical and physical properties of selected sands

	Fine sand	Lightweight sand
SiO_2(%)	86.50	57.60
Al_2O_3(%)	0.39	19.40
Fe_2O_3(%)	1.47	9.60
CaO (%)	9.42	3.40
MgO(%)	0	2.60
SO_3(%)	0	0.60
Na_2O eq. (%)	–	5.60
Loss of ignition (%)	0.24	–
Specific gravity, SSD	2.64	1.80

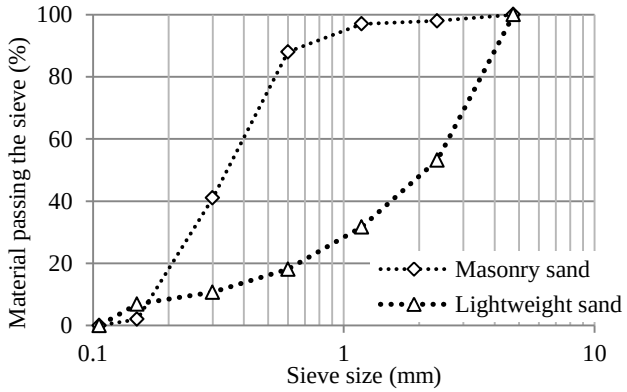

Figure S1. Grain-size distribution of fine sand and lightweight sand.

As indicated in Table 2 of the manuscript, the mixture proportions of the central points (mixtures No. 9 to 12) are provided in Table S2.

Table S2 Proportioning of the UHPC mixture of central points (unit: kg/m^3)

Code	Cement	SF	FAC	Lightweight sand	River sand	Masonry sand	HRWR	Total water	Steel fibers
FAC40SF5	663	42	367	60	615	308	12.0	171	156